Mecánica Computacional Vol. XXIV
A. Larreteguy (Editor)
Buenos Aires, Argentina, Noviembre 2005

BOND GRAPH MODELING OF INCOMPRESSIBLE THERMOFLUID FLOWS

Jorge L. Baliño

Escola Politécnica,
Universidade de São Paulo,
Av. Prof. Mello Moraes, 2231, CEP 05508-900, Cidade Universitária,
São Paulo, SP, Brazil
email: jlbalino@usp.br, web page: http://www.poli.usp.br/

Key Words: Bond Graphs, Computational Fluid Dynamics, incompressible flow, numerical methods, Galerkin formulation.

Abstract. *In this paper a Bond Graph methodology is used to model incompressible fluid flows with viscosity and heat transfer. The distinctive characteristic of these flows is the role of pressure, which doesn't behave as a state variable but as a function that must act in such a way that the resulting velocity field has divergence zero. Velocity and entropy per unit volume are used as independent variables for a single-phase, single-component flow. Time-dependent nodal values and interpolation functions are introduced to represent the flow field, from which nodal vectors of velocity and entropy are defined as Bond Graph state variables. The system of equations for the momentum equation and for the incompressibility constraint is coincident with the one obtained by using the Galerkin formulation of the problem in the Finite Element Method, in which general boundary conditions are possible through superficial forces. The integral incompressibility constraint is derived based on the integral conservation of mechanical energy. All kind of boundary conditions are handled consistently and can be represented as generalized effort or flow sources for the velocity and entropy balance equations. A procedure for causality assignment is derived for the resulting graph, satisfying the Second principle of Thermodynamics.*

1 INTRODUCTION

In recent years, it was observed an increasing interest in formulating system models in which fluid dynamic and heat transfer effects are important. In order to solve multidimensional problems with the aid of computer programs, it is important that these models can be implemented numerically. This task, main concern of the area of Computational Fluid Dynamics (CFD), is performed by systematically discretizing the continua, that is, by replacing the continuous variables by a combination of a finite set of nodal values and interpolating functions. The result is a (generally nonlinear) algebraic approximation, instead of the original differential or integro-differential problem.

The Bond Graph formalism allows for a systematic approach for representing and analyzing dynamic systems.[1] Dynamic systems belonging to different fields of knowledge like Electrodynamics, Solid Mechanics or Fluid Mechanics can be described in terms of a finite number of variables and basic elements.

1.1 Incompressible Flows

An interesting type of problems are those in which the fluid is incompressible, this is, density is constant.

When viscosity variations with temperature are small, the traditional incompressible form of the Navier-Stokes (N-S) equation is usually selected for the analysis. A set of equations (continuity, momentum and thermal energy) results with three unknowns, for which usually velocity, pressure and temperature are chosen; this is known as the *primitive-variable approach*. Other alternatives have a limitation to bi-dimensional flows (vorticity-stream function approach), or are less attractive for three-dimensional flows (vector potencial approach); consequently, the N-S equations are often solved in their primitive variable form.

For constant viscosity, the energy equation can be uncoupled, so the temperature field can be obtained after the velocity field has been computed. Since the non-linearities are related to the convective term, the attention is focused on the solution of the continuity and momentum equations.

An important characteristic of the N-S equations is that no time derivative of pressure appears. Pressure is no longer a thermophysical property, but a function that must act in such a way that the resulting velocity field has divergence zero. In an incompressible flow pressure perturbations propagate at infinite speed, obeying an elliptic, Poisson's type partial differential equation, where the source term is a function of the velocity field.

A strategy often employed for the numerical solution of the incompressible N-S equations is the *pressure correction approach*, in which a derived equation is used to determine the pressure. Typically, the momentum equations are solved for the velocity components using linearized expressions in which time-lagged values are used for the variables other than the unknown, including pressure. In this step, the obtained velocity field does not satisfy the continuity equation. Next, the solution is substituted in the discretized continuity equation and often a Poisson equation is developed for the pressure (or pressure changes), from which a new pressure field

is obtained. This pressure field is used to calculate a new velocity field until a solution is produced that satisfies both the momentum and the continuity equations. The literature on numerical schemes using the pressure correction approach is extensive, differing the methods in the algorithms used to solve the component equations and the improved pressure field.[2]

1.2 Bond Graphs and CFD

The first attempt to apply Bond Graphs in fluid dynamic systems with a systematic spatial discretization of flow fields, typical of CFD problems, appeared less than a decade ago.[3] A compressible flow was considered, although the formulation was restricted to prescribed shape functions and nodalization. Besides, heat conduction (which leads to convection-diffusion problems) was not modeled.

A few years ago, a theoretical development of a general Bond Graph approach for CFD was presented.[4] Density, entropy per unit volume and velocity were used as discretized variables for single-phase, single component flows. Time-dependent nodal values and interpolation functions were introduced to represent the flow field. Nodal vectors of mass, entropy and velocity were defined as Bond Graph state variables. It was shown that the system total energy can be represented as a three-port IC-field. The conservation of linear momentum for the nodal velocity is represented at the inertial port, while mass and entropy conservation equations are represented at the capacitive ports. All kind of boundary conditions are handled consistently and can be represented as generalized modulated sources. The methodology was successful in different applications: one-dimensional convection-diffusion,[5] one-dimensional problems with constant piecewise shape functions,[6,7] *shock tube* problem[8] and single-phase, multicomponent flows.[9,10] The motivation of this paper is the extension of the methodology described before[4] to incompressible flows.

2 TOTAL ENERGY PER UNIT VOLUME

For an incompressible fluid, the density ρ_0 is no longer a state variable. The internal energy per unit volume u_v ($u_v = \rho_0 \, \hat{u}$, where $\hat{u}$ is the internal energy per unit mass) is only a function of the entropy per unit volume s_v ($s_v = \rho_0 \, \hat{s}$, where $\hat{s}$ is the entropy per unit mass). The total energy per unit volume e_v can be written as:

$$e_v = u_v(s_v) + t_v^*(\boldsymbol{V}) \tag{1}$$

where $t_v^* = \frac{1}{2} \rho_0 \, \boldsymbol{V}^{\,2}$ is the kinetic coenergy per unit volume. The following potentials are defined:

$$\boldsymbol{p}_v = \frac{dt_v^*}{d\boldsymbol{V}} = \rho_0 \, \boldsymbol{V} \qquad ; \qquad \theta = \frac{du_v}{ds_v} \tag{2}$$

where $\boldsymbol{p}_v$ and θ are correspondingly the linear momentum per unit volume and the temperature. The time derivative of (1) can be written as:

$$\frac{\partial e_v}{\partial t} = \boldsymbol{p}_v \, . \, \frac{\partial \boldsymbol{V}}{\partial t} + \theta \, \frac{\partial s_v}{\partial t} \tag{3}$$

Since the internal energy per unit volume is only a function of the entropy per unit volume, and the kinetic coenergy per unit volume is only a function of the velocity, these two energy types can be split.

3 CONSERVATION EQUATIONS

For an incompressible fluid the mass, linear momentum and thermal energy conservation equations are:

$$\nabla . \boldsymbol{V} = 0 \tag{4}$$

$$\rho_0 \frac{\partial \boldsymbol{V}}{\partial t} = -\nabla t_v^* + \rho_0 \boldsymbol{V} \times (\nabla \times \boldsymbol{V}) - \nabla P + \rho_0 \boldsymbol{G} + \nabla . \underline{\underline{\tau}} \tag{5}$$

$$\frac{\partial u_v}{\partial t} = -\nabla . \boldsymbol{q} - \nabla u_v \, . \, \boldsymbol{V} + \nabla \boldsymbol{V} : \underline{\underline{\tau}} + \rho_0 \, \Phi \tag{6}$$

where t is the time, $\underline{\underline{\tau}}$ is the viscous stress tensor, P is the pressure, $\boldsymbol{G}$ is the force per unit mass, $\boldsymbol{q}$ is the heat flux and Φ is the heat source per unit mass. For a newtonian, incompressible fluid and assuming Fourier's law, the viscous stress and the heat flux can be written as:

$$\underline{\underline{\tau}} = \mu \left(\nabla \boldsymbol{V} + \nabla \boldsymbol{V}^T \right) \qquad ; \qquad \boldsymbol{q} = -\frac{\lambda \, \theta}{\rho_0 \, c_v} \nabla s_v \tag{7}$$

where μ, λ and c_v are correspondingly the fluid viscosity, thermal conductivity and constant volume specific heat.

4 BALANCE EQUATIONS

The balance equations are power equations (per unit volume) corresponding to each one of the terms that contributes to the time derivative of the total energy per unit volume, namely (3). Making the scalar product of (5) times the velocity and taking into account (4) and the following identities:

$$\left[\boldsymbol{V} \times (\nabla \times \boldsymbol{V}) \right] . \boldsymbol{V} = 0 \tag{8}$$

$$\left(\nabla . \underline{\underline{\tau}} \right) . \boldsymbol{V} = \nabla . \left(\underline{\underline{\tau}} \, . \, \boldsymbol{V} \right) - \nabla \boldsymbol{V} : \underline{\underline{\tau}} \tag{9}$$

we have:

$$\boldsymbol{p}_v \, . \, \frac{\partial \boldsymbol{V}}{\partial t} = \nabla . \left[\left(-P \, \underline{\underline{\mathbf{I}}} + \underline{\underline{\tau}} \right) . \boldsymbol{V} \right] - \nabla t_v^* \, . \, \boldsymbol{V} + \rho_0 \, \boldsymbol{G} \, . \, \boldsymbol{V} - \nabla \boldsymbol{V} : \underline{\underline{\tau}} \tag{10}$$

Taking into account (2) we have:

$$\theta \frac{\partial s_v}{\partial t} = -\nabla . \, \boldsymbol{q} - \theta \, \nabla s_v \, . \, \boldsymbol{V} + \rho_0 \, \Phi + \nabla \boldsymbol{V} : \underline{\underline{\tau}} \tag{11}$$

The balance equations show the power structure of the system. In the balance equations there can be identified three type of terms: divergence, coupling and source terms. The divergence

terms will take into account the power introduced in the system through the boundary conditions. The coupling term $\nabla \boldsymbol{V} : \underline{\underline{\tau}}$ represents the power transfer (mechanical energy dissipation) between the velocity and entropy equations; this coupling term appears, with opposite signs, in the balance equations. Finally, the remaining terms are regarded as power sources. Adding the balance equations, it can be easily obtained the conservation of total energy:

$$\rho_0 \frac{D\hat{e}}{Dt} = \nabla . \left[\left(-P \underline{\underline{\mathbf{I}}} + \underline{\underline{\tau}} \right) . \boldsymbol{V} - \boldsymbol{q} \right] + \rho_0 \boldsymbol{G} . \boldsymbol{V} + \rho_0 \Phi \tag{12}$$

where $\hat{e} = \hat{u} + \frac{1}{2} \boldsymbol{V}^{\,2}$ is the total energy per unit mass and $\frac{D}{Dt}$ is the material derivative.

5 DISCRETIZATION

5.1 Description of the Flow Fields

The description of the flow fields corresponding to the independent variables in the domain Ω is made in terms of a finite set of nodal values and interpolation functions, as in the Finite Element Method:[11]

$$\boldsymbol{V}(\boldsymbol{r},\, t) = \sum_{m=1}^{n_V} \boldsymbol{V}_m(t)\; \varphi_{V\,m}(\boldsymbol{r}) = \underline{\boldsymbol{V}}^T . \underline{\varphi_V} \tag{13}$$

$$s_v(\boldsymbol{r}, t) = \sum_{l=1}^{n_S} s_{v\,l}(t)\; \varphi_{s\,l}(\boldsymbol{r}) = \underline{s_v}^T . \underline{\varphi_S} \tag{14}$$

$$P(\boldsymbol{r}, t) = \sum_{k=1}^{n_P} P_k(t)\; \varphi_{P\,k}(\boldsymbol{r}) = \underline{P}^T . \underline{\varphi_P} \tag{15}$$

where $\underline{\boldsymbol{V}}$ (size n_V), $\underline{s_v}$ (size n_S) and $\underline{P}$ (size n_P) are time-dependent nodal vectors, while $\underline{\varphi_V}$, $\underline{\varphi_S}$ and $\underline{\varphi_P}$ are the corresponding nodal interpolation or shape functions.

5.2 Nodal Entropy Vector

The nodal vector of entropy is defined as:

$$\underline{S} = \underline{\underline{\Omega_S}} . \underline{s_v} \qquad ; \qquad (\Omega_S)_{l\,n} = \Omega_{S\,l}\, \delta_{l\,n} \qquad ; \qquad \Omega_{S\,l} = \int_\Omega \varphi_{S\,l}\; d\Omega \tag{16}$$

where $\underline{\underline{\Omega_S}}$ is a diagonal volume matrix associated to the entropy per unit volume. The system entropy can be obtained as:

$$S = \int_\Omega s_v\, d\Omega = \sum_{l=1}^{n_S} S_l \tag{17}$$

5.3 Total Energy

The system total energy E is defined as the sum of the internal energy U and the kinetic coenergy T^*:

$$E = U(\underline{S}) + T^*(\underline{\boldsymbol{V}}) \tag{18}$$

where:

$$E = \int_\Omega e_v \, d\Omega \qquad ; \qquad U = \int_\Omega u_v \, d\Omega \qquad ; \qquad T^* = \int_\Omega t_v^* \, d\Omega \tag{19}$$

From (19), it can be easily shown that the system kinetic coenergy can be expressed as the following bilinear form:

$$T^* = \frac{1}{2} \underline{\boldsymbol{V}}^T . \underline{\underline{M}} . \underline{\boldsymbol{V}} \tag{20}$$

where $\underline{\underline{M}}$ is the system inertia matrix:

$$(M)_{m\,n} = \rho_0 \int_\Omega \varphi_{V\,m} \, \varphi_{V\,n} \, d\Omega \tag{21}$$

We define the following potentials:

$$\underline{\boldsymbol{p}} = \frac{dT^*}{d\underline{\boldsymbol{V}}} = \underline{\underline{M}} . \underline{\boldsymbol{V}} = \int_\Omega \boldsymbol{p}_v \, \underline{\varphi_V} \, d\Omega \tag{22}$$

$$\underline{\Theta}\,(\underline{S}) = \frac{dU}{d\underline{S}} = \underline{\underline{\Omega_S}}^{-1} . \left[\int_\Omega \theta \, \underline{\varphi_S} \, d\Omega \right] \tag{23}$$

where $\underline{\boldsymbol{p}}$ and $\underline{\Theta}$ are correspondingly nodal vectors of linear momentum and temperature. The potentials defined in (22) and (23) allow to represent kinetic and internal energy storage correspondingly as an inertial (I) and a capacitive (C) multibond field, as shown in Fig. 1.

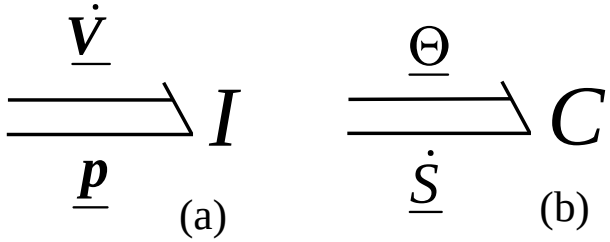

Figure 1: Inertial (a) and capacitive (b) fields, representing kinetic and internal energy storage for an incompressible fluid.

Regarding the convention used in multibonds it can be observed that, in Fig. 1 (a), the generalized effort and flow are nodal vectors whose elements are vector variables. For a three-dimensional problem, it means that this type of multibond is equivalent to $3\,n$ single bonds, being n the size of the nodal vectors involved (in this case, n_V), as shown in Fig. 2. In Fig. 1

(b), the generalized effort and flow are nodal vectors whose elements are scalar variables, which means that this type of multibond is equivalent to n (in this case, n_S) single bonds, as shown in Fig. 3.

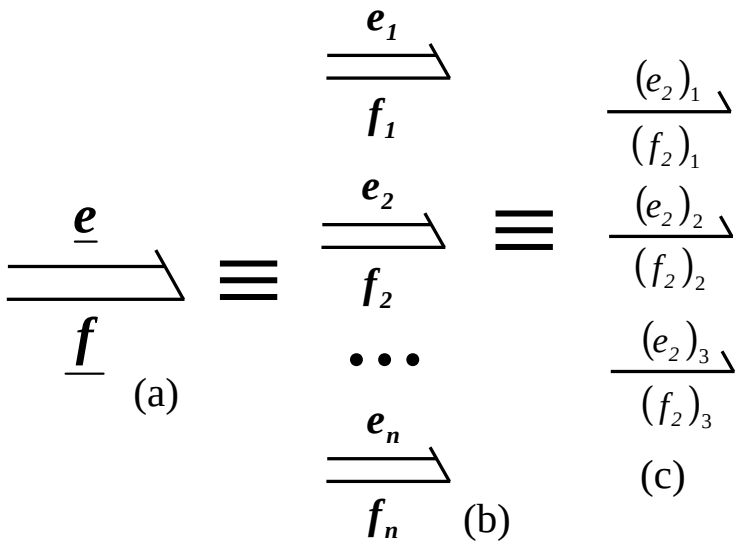

Figure 2: Multibond with nodal vector of vector variables for a three dimensional problem (a), equivalent to n multibonds of vector variables (b), each one of these equivalent to three single bonds (c).

Since the inertia matrix is constant, (22) defines a multibond transformer relating the nodal vectors of velocity and linear momentum, as shown in Fig. 4 (a), with generalized effort given by:

$$\underline{\boldsymbol{F}} = \underline{\underline{M}} \,.\, \underline{\dot{\boldsymbol{V}}} \tag{24}$$

From (24) and (22), $\underline{\boldsymbol{F}} = \underline{\dot{\boldsymbol{p}}}$ for incompressible flows. In this case, the inertia field from Fig. 1 (a) and the transformer of Fig. 4 (a) are equivalent to an inertia field in which the generalized momentum is the nodal vector of linear momentum, as shown in Fig. 4 (b).

According to (22), the nodal vector of linear momentum can be regarded as a system volume integral of the local values weighted by the velocity interpolation function. It can be easily shown that the system linear momentum can be obtained as:

$$\boldsymbol{p} = \int_\Omega \boldsymbol{p}_v \, d\Omega = \sum_{m=1}^{n_V} \boldsymbol{p}_m \tag{25}$$

According to (23), the nodal vector $\underline{\Theta}$ can be regarded as system volume average of the corresponding local value, weighted by the interpolation function.

The time derivative of (18) can be written as:

$$\dot{E} = \underline{\boldsymbol{p}}^T \,.\, \underline{\dot{\boldsymbol{V}}} + \underline{\Theta}^T \,.\, \underline{\dot{S}} \tag{26}$$

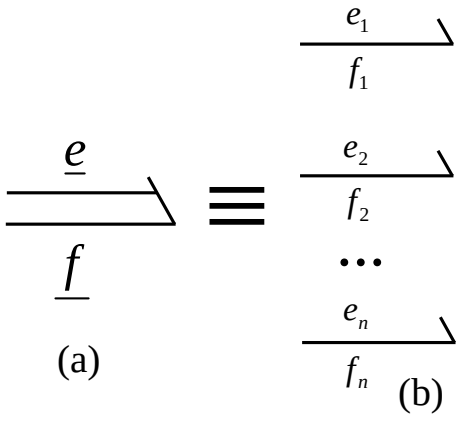

Figure 3: Multibond with nodal vector of scalar variables (a), equivalent to n single bonds (b).

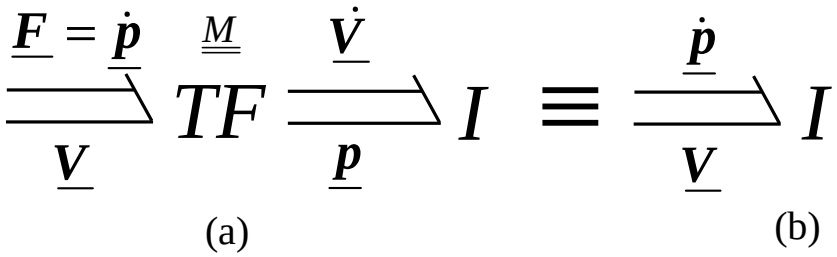

Figure 4: Multibond transformer connected to the inertial port (a), and equivalent inertia field for incompressible flow (b).

It can also be shown that the volume integrals of the left side terms of (10) and (11) can be calculated as:

$$\int_\Omega \boldsymbol{p}_v \,.\, \frac{\partial \boldsymbol{V}}{\partial t}\, d\Omega = \underline{\boldsymbol{p}}^T \,.\, \underline{\dot{\boldsymbol{V}}} \qquad ; \qquad \int_\Omega \theta\, \frac{\partial s_v}{\partial t}\, d\Omega = \underline{\Theta}^T \,.\, \underline{\dot{S}} \tag{27}$$

6 STATE EQUATIONS

6.1 Velocity Port

As it is done in the Galerkin method,[11] we multiply the momentum conservation equation by the test function $\varphi_{V\,m}$, integrate over the domain Ω and apply Green's theorem whenever necessary, obtaining:

$$\underline{\underline{M}} \,.\, \underline{\dot{\boldsymbol{V}}} = \underline{\boldsymbol{F}_V^{(\Gamma)}} + \underline{\boldsymbol{F}_P^{(\Gamma)}} + \underline{\boldsymbol{F}_G} + \underline{\boldsymbol{F}_K} + \underline{\boldsymbol{F}_R} + \underline{\boldsymbol{F}_P} - \underline{\boldsymbol{F}_V} \tag{28}$$

where:

$$\underline{\boldsymbol{F}_V^{(\Gamma)}} = \int_\Gamma \left(\underline{\underline{\tau}} \,.\, \breve{\mathbf{n}}\right) \underline{\varphi_V}\, d\Gamma \tag{29}$$

$$\underline{\boldsymbol{F}_P^{(\Gamma)}} = -\int_\Gamma P\,\underline{\varphi_V}\,\breve{\mathbf{n}}\,d\Gamma \tag{30}$$

$$\underline{\boldsymbol{F}_G} = \rho_0 \int_\Omega \boldsymbol{G}\,\underline{\varphi_V}\,d\Omega \tag{31}$$

$$\underline{\boldsymbol{F}_K} = -\int_\Omega \nabla t_v^*\,\underline{\varphi_V}\,d\Omega \tag{32}$$

$$\underline{\boldsymbol{F}_R} = \rho_0 \int_\Omega \boldsymbol{V}\times(\nabla\times\boldsymbol{V})\,\underline{\varphi_V}\,d\Omega \tag{33}$$

$$\underline{\boldsymbol{F}_P} = \int_\Omega P\,\underline{\nabla\varphi_V}\,d\Omega \tag{34}$$

$$\underline{\boldsymbol{F}_V} = \int_\Omega \underline{\underline{\tau}}\,.\,\underline{\nabla\varphi_V}\,d\Omega \tag{35}$$

Adding the nodal components of (28) it can be easily shown that the integral momentum equation is satisfied:

$$\rho_0 \int_\Omega \frac{D\boldsymbol{V}}{Dt}\,d\Omega = \int_\Gamma \left(-P\,\underline{\underline{\mathbf{I}}} + \underline{\underline{\tau}}\right).\breve{\mathbf{n}}\,d\Gamma + \rho_0\int_\Omega \boldsymbol{G}\,d\Omega \tag{36}$$

Since the interpolation function were chosen as test functions, the product $\underline{\boldsymbol{F}_X}^T.\underline{\boldsymbol{V}}$, where $\underline{\boldsymbol{F}_X}$ is any nodal vector of force, recovers the corresponding power term integrated in the system. Thus, the product $\underline{\boldsymbol{F}_V^{(\Gamma)}}^T.\underline{\boldsymbol{V}}$ recovers the power due to the flux of the viscous stress, the product $\underline{\boldsymbol{F}_V}^T.\underline{\boldsymbol{V}}$ recovers the power dissipation and the product $\underline{\boldsymbol{F}_R}^T.\underline{\boldsymbol{V}}$ is zero, because of (8).

6.2 Entropy Port

Nodal entropy weight functions $w_{Sl}(\boldsymbol{r},\,t)$ are introduced, as it is done in the Petrov-Galerkin method.[11] The nodal entropy weight functions are introduced to satisfy the power interchanged by the system through the boundary conditions, as well as to share the importance of different power terms among neighboring nodes. These functions can be used, for instance, to introduce upwind schemes in convection-diffusion problems.[5–7]

Each term of the entropy balance equation (11) is multiplied by w_{Sl}. Then, the resulting terms are integrated over the domain Ω and Gauss' theorem is applied whenever necessary, obtaining:

$$\underline{\dot{S}} = \underline{\dot{S}_Q^{(\Gamma)}} + \underline{\dot{S}_Q} + \underline{\dot{S}_F} + \underline{\dot{S}_C} + \underline{\dot{S}_V} \tag{37}$$

where:

$$\underline{\dot{S}_Q^{(\Gamma)}} = -\underline{\underline{\Theta}}^{-1}.\left[\int_\Gamma \underline{w_S}\,\boldsymbol{q}\,.\,\breve{\mathbf{n}}\,d\Gamma\right] \tag{38}$$

$$\underline{\dot{S}_Q} = \underline{\underline{\Theta}}^{-1}.\left[\int_\Omega \boldsymbol{q}\,.\,\underline{\nabla w_S}\,d\Omega\right] \tag{39}$$

$$\underline{\dot{S}_F} = \underline{\underline{\Theta}}^{-1}.\left[\rho_0 \int_\Omega \underline{w_S}\,\Phi\,d\Omega\right] \tag{40}$$

$$\underline{\dot{S}_V} = \underline{\underline{\Theta}}^{-1}.\left[\int_\Omega \underline{w_S}\,\left(\nabla \boldsymbol{V} : \underline{\underline{\tau}}\right) d\Omega\right] \tag{41}$$

$$\underline{\dot{S}_C} = -\,\underline{\underline{\Theta}}^{-1}.\left[\int_\Omega \underline{w_S}\,\theta\,\nabla s_v\,.\,\boldsymbol{V}\,d\Omega\right] \tag{42}$$

In (38) to (42) the temperature matrix $\underline{\underline{\Theta}}$ results:

$$(\Theta)_{l\,j} = \frac{1}{\Omega_{S\,j}} \int_\Omega \theta\, w_{S\,l}\, \varphi_{S\,j}\, d\Omega \tag{43}$$

The nodal vector of temperature is related to the temperature matrix as:

$$\Theta_j = \sum_{l=1}^{n_S} (\Theta)_{l\,j} \tag{44}$$

Taking into account (44) it can be verified that the product of any nodal vector of entropy rate times the nodal vector of temperature $\underline{\dot{S}_X}\,.\,\underline{\Theta}$ recovers the corresponding power integrated in the system. Thus, the product $\underline{\dot{S}_Q^{(\Gamma)}}^T.\,\underline{\Theta}$ recovers the power due to heat flux, while $\underline{\dot{S}_Q}^T.\,\underline{\Theta}$ is a power term that vanishes, because $\sum_{l=1}^{n_S} w_{S\,l} = 1$. Multiplying (37) by $\underline{\Theta}$, it can be easily shown that the integral entropy balance equation is satisfied, this is:

$$\rho_0 \int_\Omega \theta\, \frac{D\hat{s}}{Dt}\, d\Omega = -\int_\Gamma \boldsymbol{q}\,.\,\breve{\mathbf{n}}\, d\Gamma + \rho_0 \int_\Omega \Phi\, d\Omega + \int_\Omega \left(\nabla \boldsymbol{V} : \underline{\underline{\tau}}\right) d\Omega \tag{45}$$

7 DISSIPATION COUPLING MATRIX

The dissipation coupling matrix represents the power coupling (appearing in the balance equations per unit volume shown in Section 4) to a discretized level. This matrix relates generalized variables whose product gives rise to the dissipation power term, appearing in the velocity and entropy ports as:

$$\underline{\Theta}^T.\,\underline{\dot{S}_V} = \underline{\boldsymbol{F}_V}^T.\,\underline{\boldsymbol{V}} = \int_\Omega \left(\nabla \boldsymbol{V} : \underline{\underline{\tau}}\right)\, d\Omega \tag{46}$$

From (35) and (41) we have:

$$\underline{\dot{S}_V} = \left(\underline{\underline{\Theta}}^{-1}.\,\underline{\underline{\boldsymbol{M}_{SV}}}\right).\,\underline{\boldsymbol{V}} \qquad ; \qquad \underline{\boldsymbol{F}_V} = \left(\underline{\underline{\Theta}}^{-1}.\,\underline{\underline{\boldsymbol{M}_{SV}}}\right)^T.\,\underline{\Theta} \tag{47}$$

where $\underline{\underline{\boldsymbol{M}_{SV}}}$ is a rectangular matrix , with n_S rows and n_V columns, defined as:

$$(\boldsymbol{M}_{SV})_{l\,m} = \int_{\Omega} w_{S\,l} \left(\underline{\underline{\tau}} \,.\, \nabla \varphi_{V\,m} \right) d\Omega \tag{48}$$

Equation (47) defines a multibond transformer modulated by the state variables, as shown in Fig. 5, in which $\underline{\underline{\Theta}}^{-1} . \underline{\underline{\boldsymbol{M}_{SV}}}$ is the dissipation coupling matrix. Besides satisfying conservation of energy through the transformer, namely (46), it will be seen in Section 11 that the resulting causality also satisfies the Second Principle of Thermodynamics.

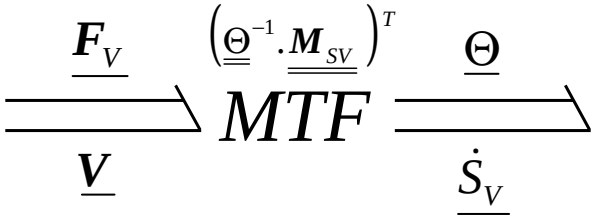

Figure 5: Modulated multibond transformer connecting the velocity and entropy ports.

8 PRESSURE AND INTEGRAL INCOMPRESSIBILITY CONSTRAINT

Making the product of (28) times $\underline{\boldsymbol{V}}$ and taking into account (8), we obtain:

$$\int_{\Omega} \frac{Dt_v^*}{Dt} \, d\Omega = \int_{\Gamma} \left[\left(-P \, \underline{\underline{\mathbf{I}}} + \underline{\underline{\tau}} \right) . \boldsymbol{V} \right] . \breve{\mathbf{n}} \, d\Gamma + \rho_0 \int_{\Omega} \boldsymbol{G} \,.\, \boldsymbol{V} \, d\Omega - \int_{\Omega} \left(\nabla \boldsymbol{V} : \underline{\underline{\tau}} \right) \, d\Omega + \underline{\boldsymbol{F}_P}^T . \underline{\boldsymbol{V}} \tag{49}$$

Comparing (10) with (49), the velocity balance equation (conservation of mechanical energy) integrated over the domain Ω is satisfied if $\underline{\boldsymbol{F}_P}^T . \underline{\boldsymbol{V}} = 0$. This power term can be expressed as:

$$\underline{\boldsymbol{F}_P}^T . \underline{\boldsymbol{V}} = \int_{\Omega} P \left(\nabla . \boldsymbol{V} \right) d\Omega = \underline{P}^T . \underline{Q} \tag{50}$$

where the nodal vector of volumetric flows $\underline{Q}$ results:

$$\underline{Q} = \int_{\Omega} \underline{\varphi_P} \left(\nabla . \boldsymbol{V} \right) d\Omega \tag{51}$$

As a consequence, the integral incompressibility condition that must satisfy the discretized velocity field is:

$$\underline{Q} = \underline{0} \tag{52}$$

The system of equations (28) and (52) is coincident with the one obtained by using the weak formulation of the problem in the Finite Element Method,[11] in which general boundary conditions are possible through the superficial forces $\underline{\boldsymbol{F}_V^{(\Gamma)}}$ and $\underline{\boldsymbol{F}_P^{(\Gamma)}}$. Adding the components of vector $\underline{Q}$, it can be verified that the integral continuity equation is satisfied, this is:

$$\int_{\Omega} (\nabla . \boldsymbol{V})\, d\Omega = \int_{\Gamma} \boldsymbol{V} . \breve{\mathbf{n}}\, d\Gamma = 0 \tag{53}$$

The power conserving transformation between the force and pressure ports is represented by a multibond transformer, as shown in Fig. 6, with relations given by:

$$\underline{\boldsymbol{F}_P} = \underline{\underline{\boldsymbol{M}_{PV}}} . \underline{P} \qquad ; \qquad \underline{Q} = \underline{\underline{\boldsymbol{M}_{PV}}}^T . \underline{\boldsymbol{V}} \tag{54}$$

where $\underline{\underline{\boldsymbol{M}_{PV}}}$ is a rectangular matrix, with n_V rows and n_P columns, defined as:

$$(\boldsymbol{M}_{PV})_{m\,k} = \int_{\Omega} \nabla\varphi_{V\,m}\, \varphi_{P\,k}\, d\Omega \tag{55}$$

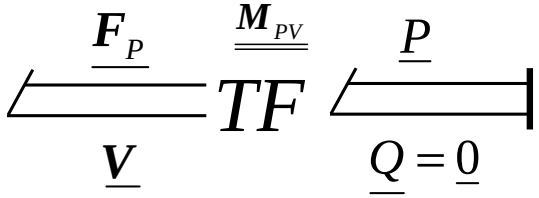

Figure 6: Multibond transformer representing the integral incompressibility constraint.

Concerning the bond corresponding to the superficial pressure force $\underline{\boldsymbol{F}_P^{(\Gamma)}}$, the power term can be written as:

$$\underline{\boldsymbol{F}_P^{(\Gamma)}}^T . \underline{\boldsymbol{V}} = -\int_{\Gamma} P\, \boldsymbol{V} . \breve{\mathbf{n}}\, d\Gamma = \underline{P}^T . \underline{Q^{(\Gamma)}} \tag{56}$$

where the nodal vector of superficial volumetric flows $\underline{Q^{(\Gamma)}}$ is defined as:

$$\underline{Q^{(\Gamma)}} = -\int_{\Gamma} \underline{\varphi_P}\, \boldsymbol{V} . \breve{\mathbf{n}}\, d\Gamma \tag{57}$$

The power conserving transformation between the superficial force and pressure is represented by a multibond transformer, as shown in Fig. 7, with relations given by:

$$\underline{\boldsymbol{F}_P^{(\Gamma)}} = \underline{\underline{\boldsymbol{M}_{PV}^{(\Gamma)}}} . \underline{P} \qquad ; \qquad \underline{Q^{(\Gamma)}} = \underline{\underline{\boldsymbol{M}_{PV}^{(\Gamma)}}}^T . \underline{\boldsymbol{V}} \tag{58}$$

where $\underline{\underline{\boldsymbol{M}_{PV}^{(\Gamma)}}}$ is a rectangular matrix, with n_V rows and n_P columns, defined as:

$$\left(\boldsymbol{M}_{PV}^{(\Gamma)}\right)_{m\,k} = -\int_{\Gamma} \varphi_{V\,m}\, \varphi_{P\,k}\, \breve{\mathbf{n}}\, d\Gamma \tag{59}$$

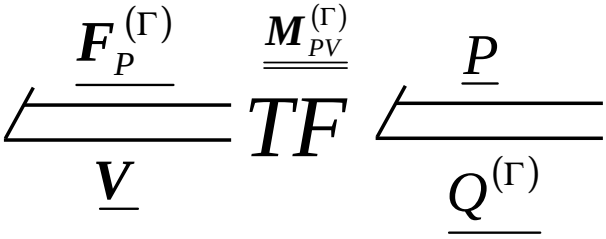

Figure 7: Multibond transformer representing the superficial pressure force.

9 SYSTEM BOND GRAPH

The system Bond Graph is shown in Fig. 8. Energy storage (kinetic and internal) are represented correspondingly by an inertial (I) and a capacitive (C) field. At the 1-junction with common $\underline{\boldsymbol{V}}$ we add all the nodal vector forces; in this way, the effort balance represents the linear momentum conservation equation for the nodal velocity values. At the 0-junction with common $\underline{\Theta}$ we add all the nodal entropy changes per unit time; in this way, the flow balance represents the thermal energy conservation equation for the nodal entropy values.

The modulated transformer connecting the 1 and 0 junctions represents the power transfer between the velocity and entropy ports, due to dissipation.

The sources S (the ones connected to the bonds with $\underline{\boldsymbol{F}_V^{(\Gamma)}}$, $\underline{\dot{S}_Q^{(\Gamma)}}$ and $\underline{Q^{(\Gamma)}}$) represent different source terms related to the boundary conditions; as it will be shown in Section 10, in each single port these sources behave as effort or flow sources, depending on the boundary conditions.

The rest of the sources, effort S_e or flow S_f (the ones connected to the bonds with $\underline{Q}$, $\underline{\boldsymbol{F}_G}$, $\underline{\boldsymbol{F}_R}$, $\underline{\boldsymbol{F}_K}$, $\underline{\dot{S}_Q}$, $\underline{\dot{S}_F}$ and $\underline{\dot{S}_C}$) represent volumetric power terms; the determination of causality for these sources and for the bonds connected to the modulated transformer MTF results from the causality extension procedure detailed in Section 11. The power input in any bond corresponding to the multibond with $\underline{Q}$ is zero, according to the integral incompressibility constraint, (52); as a consequence the causality is such that, in any of these bonds, flow is imposed to the ports connected to the transformer and the modulated source becomes a flow source S_f. The net power input (sum over the bonds) corresponding to the multibond with the rotational force $\underline{\boldsymbol{F}_R}$ is zero, because of (8). As we saw before, the net power input (sum over the bonds) corresponding to the multibond with the entropy rate $\underline{\dot{S}_Q}$ is also zero.

10 INITIAL AND BOUNDARY CONDITIONS

Initial conditions, satisfying the integral incompressibility constraint detailed in Section 8, can be written as:

$$\underline{\boldsymbol{V}}(t=0) = \underline{\boldsymbol{V}_0} \qquad ; \qquad \underline{S}(t=0) = \underline{S_0} \tag{60}$$

The boundary conditions establish relationships among the variables corresponding to the nodes located at the system surface and can be regarded (in the Bond Graph methodology) as

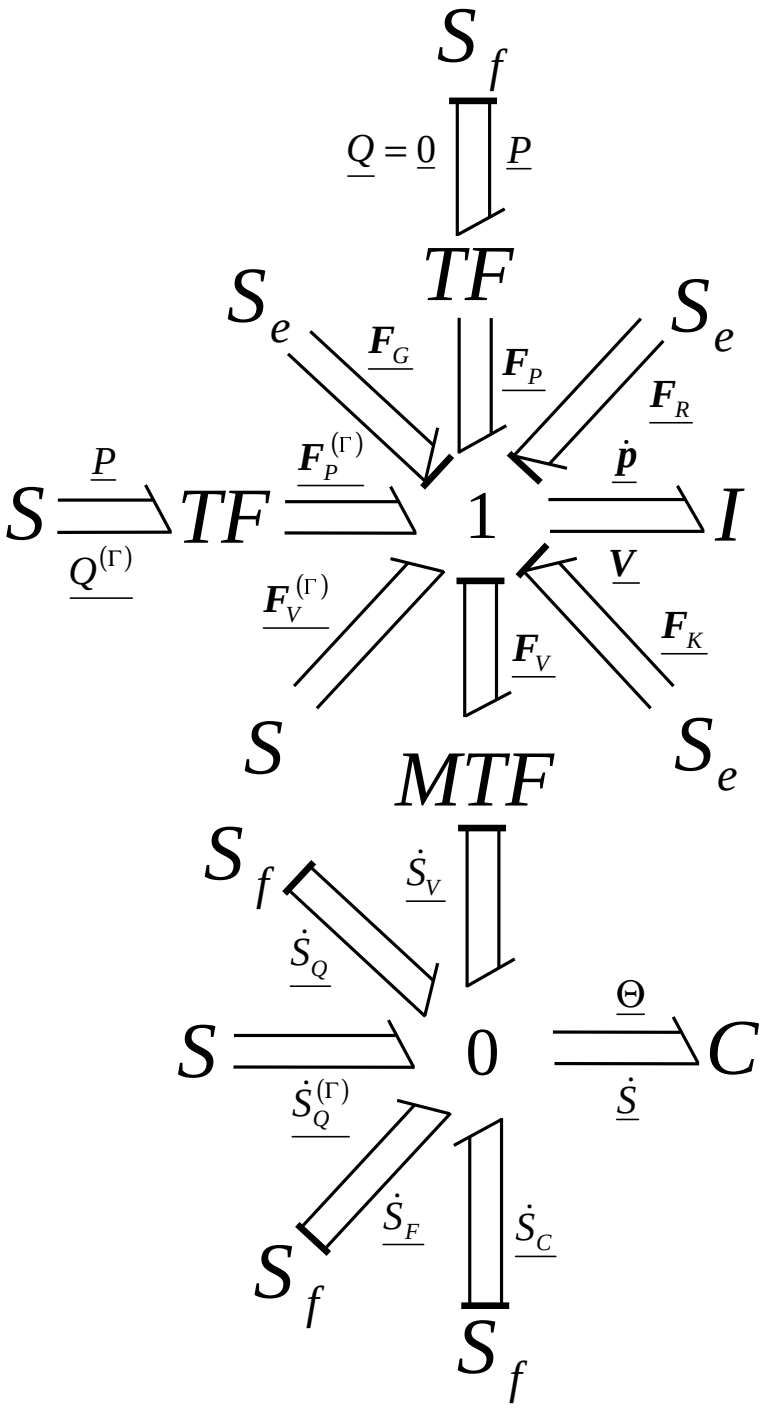

Figure 8: System Bond Graph for an incompressible fluid.

the input variables. It is necessary, for the model being mathematically well defined, that the boundary conditions allow to determine univoquely the causality for all the elements in the resulting Bond Graph.

In the following, some examples corresponding to typical boundary conditions appearing in incompressible problems and the corresponding causality extensions are discussed.

10.1 Imposed stress

The stress boundary condition can be stated as:

$$\left[\underline{\boldsymbol{\tau}}\left(\boldsymbol{r}_{\Gamma_T},\, t\right) .\, \breve{\mathbf{n}}\right] .\, \breve{\mathbf{u}}_k = \left(\tau_{\Gamma_T}\right)_k \tag{61}$$

where $\boldsymbol{r}_{\Gamma_T}$ is the position of a point belonging to the surface Γ_T, in which the stress is imposed, $\breve{\mathbf{n}}$ is the unit vector normal to Γ_T and $\breve{\mathbf{u}}_k$ is a unit vector in the k-component direction. Then, for the node m, $\left(F_{V\,m}^{(\Gamma)}\right)_k$ is imposed to the 1-junction and the corresponding source behaves as an effort source. After the causality assignment procedure of Section 11 is applied, the rest of the bonds (except the one of $(F_m)_k$) impose effort to the 1-junction, as show in Fig. 9 (a), and the inertial port results with its preferred integral causality.

10.2 Imposed velocity field

The velocity boundary condition can be stated as:

$$\boldsymbol{V}\left(\boldsymbol{r}_{\Gamma_V},\, t\right) .\, \breve{\mathbf{u}}_k = \left[V_{\Gamma_V}\left(\boldsymbol{r}_{\Gamma_V},\, t\right)\right]_k \tag{62}$$

where $\boldsymbol{r}_{\Gamma_V}$ is the position of a point belonging to the surface $\Gamma_V \subseteq \Gamma$, in which the velocity is imposed. Condition (62) is approximated by a set of n_{Γ_V} nodes located at the positions $\boldsymbol{r}_m$ ($\boldsymbol{r}_m \in \Gamma_V$, $m = 1,\, ...,\, n_{\Gamma_V}$) in which velocity is imposed. For these positions it can be written:

$$\left(V_m\right)_k = \left[V_{\Gamma_V}\left(\boldsymbol{r}_m,\, t\right)\right]_k \tag{63}$$

As a consequence, the source element connected to the bond with $\left(F_{V\,m}^{(\Gamma)}\right)_k$ behaves as a flow source. When causality is extended to the bonds connected to the 1-junction, as show in Fig. 9 (b), the rest of the bonds must impose force. After the causality assignment procedure is applied, it results a derivative causality in the corresponding inertial port.

10.3 Imposed pressure

The pressure boundary condition can be stated as:

$$P\left(\boldsymbol{r}_{\Gamma_P},\, t\right) = P_{\Gamma_P} \tag{64}$$

where $\boldsymbol{r}_{\Gamma_P}$ is the position of a point belonging to the surface Γ_P, in which the pressure is imposed. Condition (64) is approximated by a set of n_{Γ_P} pressure nodes located at the positions $\boldsymbol{r}_k$ ($\boldsymbol{r}_k \in \Gamma_P$, $k = 1,\, ...,\, n_{\Gamma_P}$) in which pressure is imposed. For these positions we can write:

$$P_k(t) = P\left(\boldsymbol{r}_k,\, t\right) \tag{65}$$

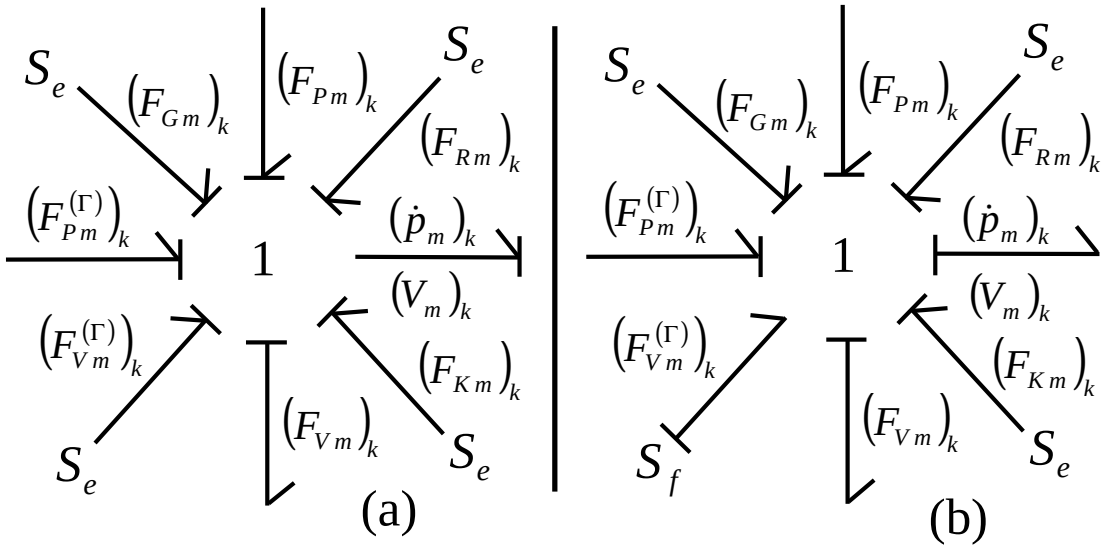

Figure 9: Causality extensions at a I-field port, integral (a) and derivative (b).

As a consequence, the sources connected to the bonds with imposed pressure behave as effort sources. Since the solution for an incompressible flow depends on pressure differences, in the case in which there are no pressure boundary conditions a source must be chosen and defined as effort source, assigning as effort the pressure reference value.

10.4 Imposed heat flux or convection

The heat flux boundary condition can be stated as:

$$\boldsymbol{q}\left(\boldsymbol{r}_{\Gamma_N},\, t\right).\breve{\mathbf{n}} = q_{\Gamma_N} \tag{66}$$

where $\boldsymbol{r}_{\Gamma_N}$ is the position of a point belonging to the surface Γ_N, in which the heat flux is imposed. Then, for the node l, $\dot{S}_{Ql}^{(\Gamma)}$ is imposed to the 0-junction and the corresponding source behaves as a flow source. After the causality assignment procedure is applied, the rest of the bonds (except the one of $\dot{S}_l$) impose flow to the 0-junction, as show in Fig. 10 (a), and the capacitive port results with its preferred integral causality.

The considerations above are valid also for the convection boundary condition, that can be stated as:

$$\boldsymbol{q}\left(\boldsymbol{r}_{\Gamma_N},\, t\right).\breve{\mathbf{n}} = H\left(\theta_{\Gamma_N} - \theta_{\Gamma\infty}\right) \tag{67}$$

where H is the heat transfer coefficient, θ_{Γ_N} is the surface temperature and $\theta_{\Gamma\infty}$ is a reference local surface temperature.

10.5 Imposed temperature

The temperature boundary condition can be stated as:

$$\theta\left(\boldsymbol{r}_{\Gamma_D},\, t\right) = \theta_{\Gamma_D} \tag{68}$$

where $\boldsymbol{r}_{\Gamma_D}$ is the position of a point belonging to the surface Γ_D, in which the temperature is imposed. Since $\theta = \theta\left(s_v\right)$, (68) can be transformed to:

$$s_v\left(\boldsymbol{r}_{\Gamma_D},\, t\right) = s_{v\,\Gamma_D} \tag{69}$$

Taking into account (16), condition (69) is approximated by a set of n_{Γ_D} entropy nodes located at the positions $\boldsymbol{r}_l$ ($\boldsymbol{r}_l \in \Gamma_D$, $l = 1,\, ...,\, n_{\Gamma_D}$) in which now entropy per unit volume is imposed. For these positions we can write:

$$s_{v\,l}(t) = s_{v\,l}\left(\boldsymbol{r}_l,\, t\right) \qquad ; \qquad \dot{S}_l(t) = \Omega_{S\,l}\, \dot{s}_{v\,l}(t) \tag{70}$$

As a consequence, $\dot{S}_l$ is an input to the 0-junction, resulting a derivative causality for the corresponding port of the C-field; to accomplish this, the sources connected to the bonds with imposed temperature behave as effort sources, resulting the causality extension shown in Fig. 10 (b).

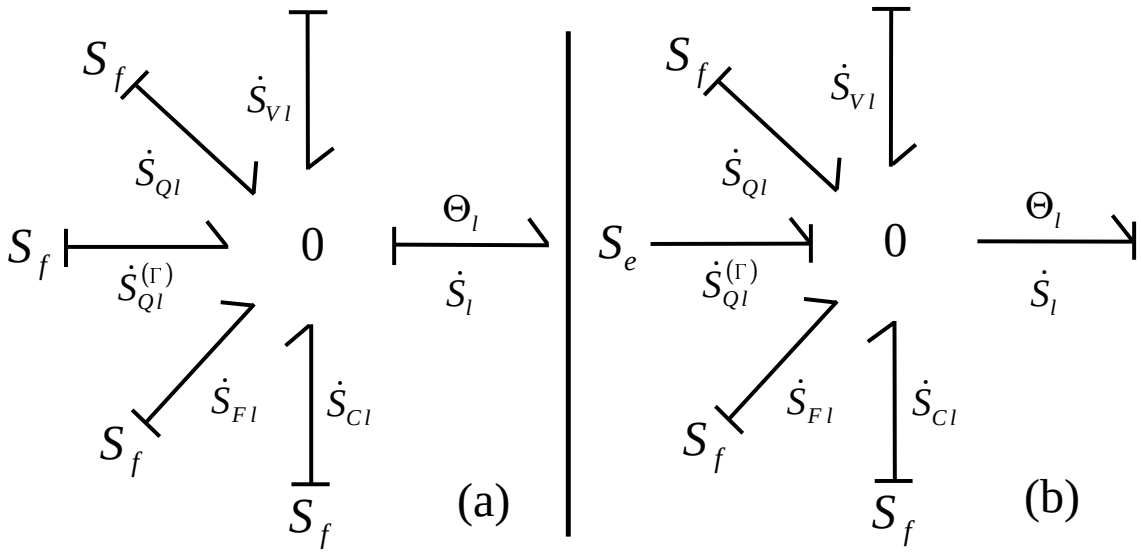

Figure 10: Causality extensions at a C-field port, integral (a) and derivative (b).

11 PROCEDURE FOR CAUSALITY ASSIGNMENT

A sequencial causal assignment procedure exists in Bond Graphs.[1] Sources are chosen first, the required causality is assigned and the causal implications are extended through the graph as far as possible, using the constraint elements (in this case 0-junctions, 1-junctions and transformers). Then, the ports corresponding to the storage elements (in this case I-field and C-field) are

chosen, integral causality is assigned and, again, the causal implications are extended through the graph as far as possible.

Regarding causality extension through the MTF and TF elements, the constitutive laws are sets of linear relationships among the variables involved. Thus, causality can be extended for a bond with a variable only when the bonds corresponding to the rest of the variables in the linear relationship have assigned causalities.

It is worth noting that, since the interpolation and weight functions are zero at the surface Γ, causality is assigned by definition at the bonds corresponding to inner nodes. Thus, a zero-effort source is connected to an inner $\boldsymbol{F}_{V\,m}^{(\Gamma)}$ or $\boldsymbol{F}_{P\,m}^{(\Gamma)}$ and a zero-flow source is connected to an inner $Q_k^{(\Gamma)}$ or $\dot{S}_{Q\,l}^{(\Gamma)}$.

Since there are only energy storing and conserving elements, all bonds should have causality assigned after the procedure detailed above. The order of the system is the number of bonds connected to the energy storing elements, resulting with integral causality. This causality procedure can be implemented automatically, knowing the connectivity of the computational grid, as a way of checking the correctness of the boundary conditions in the problem. As a consequence of the causality extension, the sources connected to the bonds with $\underline{\boldsymbol{F}_G}$, $\underline{\boldsymbol{F}_R}$ and $\underline{\boldsymbol{F}_K}$ always behave as effort sources, and the sources connected to the bonds with $\underline{\dot{S}_Q}$, $\underline{\dot{S}_F}$ and $\underline{\dot{S}_C}$ always behave as flow sources. Besides, causality for the bonds connected to the modulated transformer (the ones with $\underline{\boldsymbol{F}_V}$ and $\underline{\dot{S}_V}$) is also defined, always resulting $\underline{\boldsymbol{V}}$ an input to the transformer and $\underline{\dot{S}_V}$ an output; this indicates that fluid motion generates the irreversible entropy rate, in agreement with the Second Principle of Thermodynamics. Besides, $\underline{\Theta}$ always results an input to the transformer and $\underline{\boldsymbol{F}_V}$ an output, indicating that temperature influences the viscous force through the temperature dependence of viscosity.

12 CONCLUSIONS

In this paper, a Bond Graph methodology was used to model incompressible fluid flows with viscosity and heat transfer. The resulting representation shows the role of pressure as external function acting to satisfy the incompressibility condition and the coupling between the inertial and thermal ports through the power dissipation term. The system of equations for the momentum equation and for the incompressibility constraint is coincident with the one obtained by using the Galerkin formulation of the problem in the Finite Element Method, in which general boundary conditions are possible through superficial forces. The integral incompressibility constraint is derived based on the integral conservation of mechanical energy. All kind of boundary conditions are handled consistently and can be represented as generalized effort or flow sources for the velocity and entropy balance equations. A procedure for causality assignment is derived for the resulting graph, satisfying the Second principle of Thermodynamics. This causality procedure can be implemented automatically, knowing the connectivity of the computational grid, as a way of checking the correctness of the boundary conditions in the problem.

ACKNOWLEDGMENTS

The author wishes to thank "Conselho Nacional de Desenvolvimento Científico e Tecnológico" (CNPq, Brazil) for the financial support as Scientific Productivity (PQ) Scholar and Visiting Researcher (2001-2003) at Instituto de Pesquisas Energéticas e Nucleares (São Paulo, Brazil), where part of this work was done.

REFERENCES

[1] Karnopp, D. C., Margolis, D. L. & Rosenberg, R. C., *System Dynamics. Modeling and Simulation of Mechatronic System*, 3d Ed., Wiley Interscience, ISBN 0-471-33301-8, 2000.

[2] Tannehill, J. C., Anderson, D. A. & Pletcher, R. H., *Computational Fluid Mechanics and Heat Transfer*, Taylor & Francis, ISBN 1-56032-046-X, 1997.

[3] Fahrenthold, E. P. & Venkataraman, M., Eulerian Bond Graphs for Fluid Continuum Dynamics Modeling, *ASME Journal of Dynamic Systems, Measurement, and Control*, vol. 118, pp. 48-57, 1996.

[4] Baliño, J. L., Larreteguy, A. E. & Gandolfo, E. F., A General Bond Graph Approach for Computational Fluid Dynamics. Part I: Theory, *2001 International Conference on Bond Graph Modeling and Simulation (ICBGM'2001)*, The Society for Computer Simulation, pp. 41-46. ISBN 1-56555-221-0, 2001.

[5] Gandolfo, E. F., Larreteguy, A. E. & Baliño, J. L., A General Bond Graph Approach for Computational Fluid Dynamics. Part II: Applications, *2001 International Conference on Bond Graph Modeling and Simulation (ICBGM'2001)*, The Society for Computer Simulation, pp. 47-52. ISBN 1-56555-221-0, 2001.

[6] Baliño, J. L., Bond-Graph Approach for Computational Fluid Dynamics: a Comparison with other Numerical Methods, *Second IEEE International Conference on System, Man and Cybernetics (SMC'02),* Paper TA1B3 (in CD, IEEE No. 02CH37349C, ISBN 0-7803-7438-X), 6 p., 2002.

[7] Baliño, J. L., Bond-Graph Formulation of CFD Problems with Constant Piecewise Shape Functions, *International Journal of Heat and Technology*, vol. 21, 1, pp. 59-66, 2003.

[8] Gandolfo Raso, E. F., Larreteguy, A. E. & Baliño, J. L., Bond-Graph Modeling of 1-D Compressible Flows, *Second IEEE International Conference on System, Man and Cybernetics (SMC'02),* Paper TA1B4 (in CD, IEEE No. 02CH37349C, ISBN 0-7803-7438-X), 6 p., 2002.

[9] Baliño, J. L., "BG-CFD Methodology for Multicomponent Solutions. Part I: Multivelocity Model", *2003 International Conference on Bond Graph Modeling and Simulation (ICBGM'2003)*, The Society for Computer Simulation, pp. 41-46, 2003.

[10] Baliño, J. L., "BG-CFD Methodology for Multicomponent Solutions. Part II: Diffusion Model", *2003 International Conference on Bond Graph Modeling and Simulation (ICBGM'2003),* The Society for Computer Simulation, pp. 47-52, 2003.

[11] Cuvelier, C., Segal, A. & van Steenhoven, A. A., *Finite Element Methods and Navier-Stokes Equations*, D. Reidel Publishing Company, Holland, 1986.